

Assessment of Plastic Flow and Fracture Properties with Small Specimens Test Techniques for IFMIF-Designed Specimens

P. Spätig 1), E. N. Campitelli 2), R. Bonadé 1), N. Baluc 1)

1) Fusion Technology-Materials, CRPP EPFL, Association EURATOM-Confédération Suisse, 5232 Villigen PSI, Switzerland

2) Laboratory for Materials Behavior, Nuclear Energy and Safety Research Department, 5232 Villigen PSI, Switzerland

e-mail contact of main author: philippe.spatig@psi.ch

Abstract. The primary mission of the International Fusion Material Irradiation Facility (IFMIF) is to generate a material database to be used for the design of various components, for the licensing and for the assessment of the safe operation of a demonstration fusion reactor. IFMIF is an accelerator-based high-energy neutron source whose irradiation volume is quite limited (0.5 l for the high fluence volume). This requires the use of small specimens to measure the irradiation-induced changes on the physical and mechanical properties of materials. In this paper, we developed finite element models to better analyze the results obtained with two different small specimen test techniques applied to the tempered martensitic steel F82H-mod. First, one model was used to reconstruct the load-deflection curves of small ball punch tests, which are usually used to extract standard tensile parameters. It was shown that a reasonable assessment of the overall plastic flow can be done with small ball punch tests. Second, we investigated the stress field sensitivity at a crack tip to the constitutive behavior, for a crack modeled in plane strain, small-scale yielding and fracture mode I conditions. Based upon a local criterion for cleavage, that appears to be the basis to account for the size and geometry effects on fracture toughness, we showed that the details of the constitutive properties play a key role in modeling the irradiation-induced fracture toughness changes. Consequently, we suggest that much more attention and efforts have to be paid in investigating the post-yield behavior of the irradiated specimens and, in order to reach this goal, we recommend the use of not only tensile specimens but also that of compression ones in the IFMIF irradiation matrices.

1. Introduction

The aggressive irradiation environment of a fusion reactor will lead to very specific material problems. These problems have been continuously addressed but many challenging issues remain to be solved in order to operate a power generating fusion reactor. Indeed, while important progresses in physics of fusion plasma have been accomplished, efforts are still necessary to better understand the irradiation effects on all the identified material candidates but also on the materials under development that will be close to the neutron flux escaping the burning plasma. These materials will undergo severe neutron fluence resulting in significant neutron-induced changes in their chemical, physical and mechanical properties. Up to now, the material fusion research community has made extensively use of fission neutron irradiation, e.g. [1,2] and/or accelerator facilities [3] to investigate the effects of irradiation on materials. As a matter of fact, the overall fusion material development has been guided by the results of irradiations whose neutron spectra do not reflect that of a fusion reactor environment. The maximum neutron energy available from a fast reactor is about 2 MeV only, leaving open all the issues related to the irradiation damage produced by the high energy neutron range of the fusion spectra, which reaches 14 MeV resulting from the deuteron-triton reactions. One specific issue related to the fusion neutron spectrum is the production of gaseous impurities (helium and hydrogen isotopes) in the material bulk simultaneously with the creation of atomic displacement damage. The extended exposures of the first wall of DEMO reactor will produce about 20 displacement per atoms per full power year (dpa/FPY), 180 atom parts per million of helium per FPY (appm/FPW) and 709 hydrogen appm/FPY [4]. Despite all the material fusion development based on the great deal of irradiation data collected over the years from fission neutron sources and accelerator based facilities, the limits of employing these types of irradiation have been identified. First, the results and conclusions obtained from a given neutron spectrum can be transferred only up to some extent to that of the fusion reactor. For instance, the effect of the correct ratios of He/dpa and H/dpa along with the appropriate primary recoil spectrum on the irradiation-

induced changes can certainly not be properly inferred from fission neutron spectra or any other irradiation experiment. Second, there will be always an intrinsic issue of reliability as long as no experimental validation has been performed to prove the validity of the data transfer. As a consequence, there is a fundamental need to build an intense high energy neutron source to serve, on the one hand, as a tool for fundamental investigations on the current material candidates as well as for the development of new and emerging materials and, on the other hand, to qualify materials for the design, the construction and the operation of a demonstration reactor.

2. The International Fusion Material Irradiation Facility

The details of the International Fusion Materials Irradiation Facility (IFMIF) design, the description of its major components and a discussion of its suitability for fusion materials research can be found in [5]. We briefly summarize hereafter the main characteristics of the facility. The neutrons are produced by stripping the protons from two 40 MeV deuteron beams in a liquid lithium target through the nuclear reactions ${}^7\text{Li}(d,2n){}^7\text{Be}$, ${}^6\text{Li}(d,n){}^7\text{Be}$. This choice is mediated by the desire to reproduce as close as possible the irradiation damage conditions occurring in the first wall and breeding blanket of a fusion reactor. The irradiation volume is located behind a stable liquid Li jet onto which two 125 mA deuteron beams are delivered. The high anisotropic (forward directed) neutron emission of the stripping process generates a rather high flux but in a relatively small useful irradiation volume. This volume is subdivided into three regions: i) the high flux test region ii) the medium flux region and iii) the low flux test region. The irradiation damage production in terms of displacement per atom (dpa) in these regions in a full power year (fpy) of operation is respectively, 20-55 dpa/fpy, 1-20 dpa/fpy and 0.1-1 dpa/fpy. In its current design, the high-flux, medium-flux and low-flux irradiation volumes are respectively of the order of 0.5 liter, 6 liters and 100 liters. In the high-flux region, mainly reduced activation materials for the first wall and blanket will be irradiated in instrumented capsules. The specimens will be tested after irradiation in hot cells. Among the materials foreseen to be irradiated in this region, we mention the tempered martensitic and the oxide dispersion strengthened steels, the vanadium alloys, the SiC_f-SiC composites, the refractory metals and alloys. Twelve separated rigs have been designed in which the irradiation temperature will be independently controlled between 250°C and 1100°C. The medium and low flux volumes will be devoted to fully instrumented in-situ tests such as creep fatigue, crack growth tests, stress corrosion tests, radiation induced conductivity, electrical degradation, tritium diffusion and release experiments. The materials concerned by these last experiments are ceramic insulators, rf-windows, ceramic breeder materials, Be-neutron multipliers and superconducting materials.

In order to use effectively the irradiation volume of the high flux volume in particular, specimens as well as the corresponding test techniques have to be miniaturized. The miniaturization of the specimens is also driven by the need of reducing the strong neutron flux gradient intrinsic to this type of source and therefore to obtain a reasonable irradiation damage homogeneity through a given specimen. In addition, it is also highly desirable to miniaturize the specimens from the point of view of handling, testing and managing radioactive materials. Over the last decades, numerous techniques applied to non-standard specimens have been developed to extract a host of mechanical and physical properties and to benchmark them with respect to the standard mechanical testing methods. Reviews and recommendations for small specimen techniques have been published e.g. [6,7]. A review of all the miniaturized and sub-sized specimens foreseen for IFMIF can be found in [8]. Among these techniques, some are simply based upon a scaling-down of the standard counterparts (tensile, fatigue, fracture toughness, for example). Other non-standard techniques have also emerged like for instance the small ball punch that we discuss hereafter. On a phenomenological basis, correlations between parameters obtained from the non-standard techniques with the usual parameters measured on standards tests have been established. However, there still remains some lack of understanding of the underlying physical processes that control the various calibration factors and their material and irradiation dependence. In order to gain insight into these processes, modeling, in the

broadest sense of the term, constitutes an inseparable tool for the correct interpretation of the results. In this line of thinking, we developed finite element models that we applied to investigate the plastic flow properties from ball punch tests and to study the influence of the constitutive behavior on the attainment of a local criterion for cleavage, criterion often considered to account for the size/geometry effects of the specimens on fracture toughness.

3. Plastic flow assessment from small ball punch tests

The small ball punch (SPT) tests have been developed to extract the tensile and fracture properties [9] and to assess the so-called ductile to brittle transition temperature [10]. In *FIG. 1*, the ball punch test experimental device is presented. It consists in deforming a center-loaded clamped disk with a spherical puncher; the load-displacement curve is then recorded. The spherical puncher is a 0.5 mm radius (R1) hard steel ball. The ball is pushed with a rod through a 1 mm hole in the upper die (D1) (a small tolerance of 0.05 mm and oil lubrication are necessary). The diameter of the hole in the lower die is 1.5 mm (D2) having a machined round billet radius of 0.2 mm (R2). The sample (in black) is a disc of 3 mm diameter (D3) and a thickness varying between 0.23 and 0.27 mm approximately (T). More details about the experimental procedure can be found in [11]. Using ABAQUS 6.4-1 code, a finite element model was developed and validated with two different steels (austenitic and tempered martensitic) [11]. Making use of our finite element model, we discuss below the expectations and limitations of the ball punch test technique in assessing the potential irradiation-induced changes in the constitutive behavior. Let us first recall that, in order to simulate a SPT curve, it is necessary to assign a constitutive behavior to the sample disk in the form of a uniaxial true stress–plastic true strain relationship, $\sigma(\epsilon_p)$. Actually, the ABAQUS code requires this input to model the multiaxial stress state that develops in the

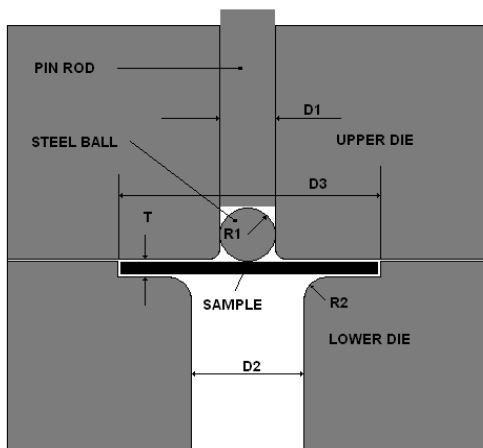


FIG. 1 Experimental ball punch test device

deformed disk using the von Mises stress potential and associated J_2 flow rule. Thus, the fundamental idea of modeling the SPT curves obtained on irradiated disks is to determine, with a series of successive simulations, a true stress - true strain relationship that allows reconstruction of the SPT curve. Let us emphasize that, after irradiation, the true stress - true strain relationship can usually not be readily established by conventional tensile test owing to the onset of necking taking place at very low strain, preventing the assessment of the post-yield behavior. In the following, we focus our attention on the behavior of the 7-9Cr class of reduced activation tempered martensitic steel, using the F82H-mod steel, produced in the framework of material development for fusion structural applications.

A typical experimental SPT load-deflection curve obtained at room temperature is shown in *FIG. 3*. Along with the experimental data, we present five simulated curves, among which two deal with the constitutive behaviors of this steel in the unirradiated condition and three are related to possible constitutive behavior that may result from irradiation-induced changes. Therefore, five specific true stress–true strain relationships have been employed to calculate the corresponding five SPT curves in *FIG. 3*. These true stress–true strain relationship are shown in *FIG. 2*.

Let us discuss first the curves obtained for the unirradiated material. The two $\sigma(\epsilon_p)$ curves for the unirradiated case were obtained by extrapolating the experimental standard tensile curve, whose true uniform strain is limited to 5%. We have already demonstrated that the constitutive behavior of a variety of tempered martensitic alloys can be successfully described in the framework of a simplified model of net storage of dislocations with plastic strain [12,13]. In this model, the increase of the post-yield component of the flow stress σ_{pl}

scales with $\rho^{1/2}$, where ρ is the total dislocation density. When the storage rate of dislocations balances the annihilation rate, the net storage is zero and the flow stress does not increase any more. Hence, within the framework of this simplified model, a saturation stress is expected. The corresponding $\sigma(\epsilon_p)$ curve is plotted in blue in FIG. 3. The red curve in FIG. 3 was obtained by extending the curve beyond necking with a linear slope [11]. Simulating the SPT curves with one or the other of stress-strain relationships assigned to the disk leads to a significant difference in the quality of the fit at deflections larger than 0.4 mm. Clearly, an excellent agreement between the simulation and the experimental SPT curves was found when using the $\sigma(\epsilon_p)$ curve without saturation. In fact, the maximum load and the deflection at maximum load were well reproduced while the $\sigma(\epsilon_p)$ curve with saturation failed to satisfactorily simulate the SPT curve at deflections larger than 0.4 mm. It must be underscored here that the SPT curves permit to sample intermediate to large strains, about 60% in terms of equivalent plastic strain at maximum load. Such strains are much larger than those measured by tensile tests. Therefore, the small ball punch test technique, when used in conjunction with finite element modeling, allows evaluation of the $\sigma(\epsilon_p)$ curve over a plastic strain range that has not been explored yet. From the simulations of the unirradiated F82H-mod punch curves, we concluded that a linear strain-hardening stage beyond necking controls the plastic flow of the tempered martensitic steel.

We have studied the effect of irradiation hardening on the shape of the SPT curves by constructing three different true stress-true strain curves representing possible constitutive behaviors of the irradiated F82H-mod steel. We arbitrarily selected an irradiation hardening (difference between the yield stresses of the unirradiated and irradiated material) of 300 MPa and constructed three different post-yield behaviors. For the first one, the same strain-hardening as that of the unirradiated material was chosen, the second one accounts for a loss of strain-hardening and the third one considers an initial softening of 100 MPa over the initial 5 % of plastic strain followed by a moderate strain-hardening regime identical to that of the unirradiated case above 5 %. For an in-depth discussion of the origin of such a softening and subsequent moderate strain-hardening, we refer to [14]. In FIG. 2, these three

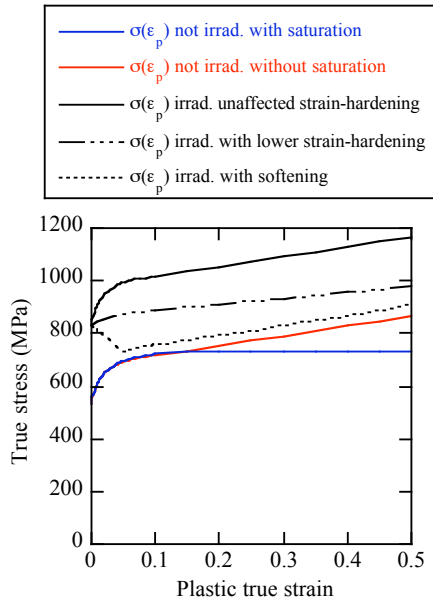


FIG. 2 Five different constitutive behaviors used as input to simulate the corresponding SPT load-deflection curves

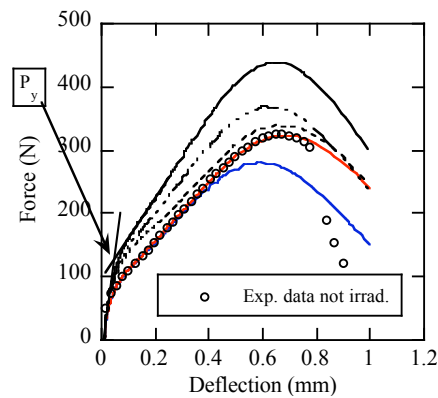


FIG. 3 Five simulated SPT load-deflection curves and one experimental curve obtained in the unirradiated condition. The colors correspond to those of the $\sigma(\epsilon_p)$ curves of figure 2 used as input for the simulations

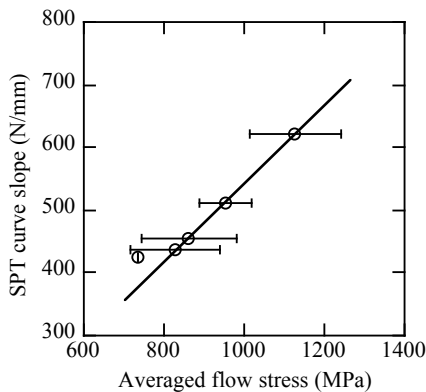


FIG. 4 Correlation between the SPT curve slope and the averaged flow stress determined between $\varepsilon = 0.1$ and 0.8 .

curves are referred as to *unaffected strain-hardening curve*, *lower strain-hardening curve*, and *with softening curve* respectively. The SPT curves calculated after having assigned these three constitutive behaviors to the punch disk are plotted in FIG. 3. Interestingly, it is observed that the load P_y , determined by the intersection of the two slopes of the load-displacement curve drawn on both side of the yielding zone, is practically independent of the post-yield behavior. This fact confirms a previous observation we made [11], *i.e.*, that P_y is mainly mediated by the yield stress $\sigma_{0.2}$. Furthermore, this also supports the use of a simple and direct calibration between P_y and $\sigma_{0.2}$. Consequently, it is reasonable to estimate the irradiation hardening from the P_y increase itself provided that a good calibration is established. As far as the post-yield behavior is concerned, it can be stated that its major role is reflected in the slope of the load-deflection curve beyond 0.2 mm. In the deflection range 0.2 mm up to 0.6 mm, the equivalent plastic strain in the disk, while not uniform at all in the disk, varies from about 0.1 to 0.6 . Looking at the $\sigma(\varepsilon_p)$ curve, in FIG. 2, it can be seen that in this strain range, the flow stress increase is moderate. Using a very crude approximation, albeit quite reasonable, the material can be regarded as deforming at a constant averaged flow stress over the strain range 0.1 - 0.6 . For the *unaffected strain-hardening curve* for instance, the averaged flow stress is about $1100 \text{ MPa} \pm 100 \text{ MPa}$ over the strain range 0.1 - 0.6 . Actually, the slope of the SPT load-deflection curve beyond 0.2 mm tends to scale with the averaged flow stress over the strain range 0.1 - 0.6 as it can be seen in FIG. 4. Thus, these slopes can be seen as the signature of the averaged strain-hardening capacity of the materials defined as the difference between the averaged flow stress and the yield stress.

Finally we would like to emphasize the following point. As already mentioned, the simple uniaxial $\sigma(\varepsilon_p)$ relationships cannot be obtained by tensile tests on irradiated materials owing to the occurrence of necking at small strain. Thus, in principle, a so-called inverse methodology has to be used, where the $\sigma(\varepsilon_p)$ curves are adjusted until a good fitting of the SPT curve is obtained. Following the above discussion, it is believed that the irradiation hardening can be satisfactorily obtained from the P_y - $\sigma_{0.2}$ calibration as well as the average strain-hardening capacity while the fine details of the $\sigma(\varepsilon_p)$ shape may certainly not be unambiguously extracted.

4. Effect of the constitutive behavior on fracture toughness

The tempered martensitic steels, like the F82H-mod, undergo a so-called ductile to brittle fracture mode transition from high-temperature microvoid coalescence to low-temperature cleavage [15]. As a consequence of neutron irradiation, the transition between the ductile and brittle regimes is shifted to higher temperatures. It is therefore of primary importance to characterize both the fracture properties of the unirradiated materials and to develop a methodology, based upon an understanding of the fundamental mechanisms, to assess the changes in fracture toughness under irradiation in order to safely manage reactor structures. As mentioned above, the fusion reactor structural materials will be qualified after irradiation in IFMIF. Consequently, fracture toughness data obtained *only* on sub-sized specimens, which *do not* meet the usual requirements of the ASTM standards, will have to be considered in the material database for designers. In other words, the standard fracture mechanics does not apply and models have to be developed that account for the size and geometry of the specimens on fracture toughness. This can be successively achieved only if strong efforts are done to better understand the whole sequence of micro- to macro-mechanisms controlling fracture. Modeling has become a key element that must be

integrated in the analysis of the experimental results. Of course, modeling has to be understood at a multiscale level where, at the continuum level, finite element analysis is a well appropriate tool. It is evidently not possible to discuss here all the details of the models currently used to account for the specimen size and geometry effects on fracture toughness. However, we briefly remind the underlining ideas of the methodology and we address only one specific point in this section.

In order to characterize the fracture toughness in the brittle regime, we can make use of the so-called local approach to cleavage to deal with the size/geometry problem. This approach is described in details in the work of Nevalainen and Dodds [16] where the model for cleavage requires the attainment of a critical stress σ^* within a critical stressed volume V^* to trigger cleavage. Other models based on the same general idea have also been used to account for the constraint loss effect on fracture toughness. While differing in the details, they involve a critical stress σ^* but acting over a critical distance λ^* or a critical area A^* [17,18]. Applications of these simple models have been successful in predicting fracture toughness in the transition region for various alloys. In particular, the constraint adjustments have been recently applied to the existing fracture toughness database of the F82H-mod steel in the transition with the ultimate goal of using a similar master curve approach as that developed for the reactor pressure vessel steel [19].

In this study, we investigate the possible effects of the irradiation hardening (increase of the yield stress) and of the post-yield behavior on the critical applied stress intensity factor necessary for the attainment of the critical condition for cleavage. In order to do so, we simulate the stress/strain fields ahead of a crack tip for plane strain and elastic-plastic small-scale yielding conditions (SSY). A fully circular model, based upon the modified boundary layer model, that contains a small notch radius ρ_0 in the middle was built, in a quite similar way as the semi-circular model described in [20]. The opening of the crack was performed in mode I by imposing the standard elastic displacements, Δx and Δy , of the nodes on the outer circular boundary and considering a T-stress equal to zero. Δx and Δy are written as:

$$\Delta x = K \frac{1+\nu}{E} \sqrt{\frac{R}{2\pi}} \cos\left(\frac{\theta}{2}\right) (3-4\nu - \cos\theta) \quad \Delta y = K \frac{1+\nu}{E} \sqrt{\frac{R}{2\pi}} \sin\left(\frac{\theta}{2}\right) (3-4\nu - \cos\theta)$$

where r is the radial distance from the crack tip and θ is the angle between the crack plane and the direction to the node, ν is the Poisson ratio and E the Young modulus. Note that the imposed displacements scale with the applied stress intensity factor K . 2D linear reduced integration elements were used. To limit the effect of the initial tip radius on the stress field at the crack tip, we ran simulations such that the crack tip opening displacement δ assures that the ratio δ/ρ_0 is larger than 4.

For the unirradiated F82H-mod steel, the fracture toughness in SSY condition is about $100 \text{ MPa m}^{1/2}$ at 170 K, temperature at which we ran a series of simulations. The corresponding measured constitutive behavior in the unirradiated condition is presented in *FIG. 5*. The necking begins at 0.05 and then the curve is simply linearly extrapolated. We selected three possible hypothetical true stress-true strain curves for the irradiated condition. All the three curves exhibit an irradiation hardening of 100 MPa but different post-yield behaviors. In the first case, the strain-hardening is not affected by irradiation. In the second case, the curves shows a Lüders-type strain region without strain-hardening up to 0.03 followed by the same strain-hardening law as that of the unirradiated material. In the third case, we consider a moderate softening (-50 MPa) over a strain of 0.03 also followed by the same strain-hardening law as that of the unirradiated material. As mentioned, the fracture toughness at 170 K is about $100 \text{ MPa m}^{1/2}$ so we imposed the corresponding elastic displacement field on the outer boundary of the mesh and assigned the $\sigma(\epsilon_p)$ unirradiated curve as the constitutive behavior of the material. Then, we assume that the local critical condition for cleavage is given by $\sigma^* = 2000 \text{ MPa}$ acting over an area $A^* = 1 \times 10^{-8} \text{ m}^2$. These last values for the (σ^* - A^*) criterion are quite similar to those already used for the F82H-mod steel to model the fracture toughness-temperature curve [18]. Then, we simulate the stress fields that develop

at the crack when one or the other of the three constitutive behaviors for the irradiated materials was selected and we search the required applied stress intensity factor K to reach the cleavage condition σ^*-A^* . The results are summarized in Table I below where the strong influence of the post-yield behavior on the attainment of σ^*-A^* can be clearly seen. Therefore, it is of a prime importance to establish the true stress-true strain relationship over a significant strain range (about 0.05). This is particularly evident if we want to predict the fracture toughness change after irradiation based upon a σ^*-A^* criterion. Unfortunately, we already mentioned that the tensile testing of the irradiated specimens does not allow getting this information due to the necking at low strain. Consequently, we recommend foreseeing in the IFMIF specimen matrices the inclusion of new type of specimens like compression or torsion ones, which would permit to investigate the true stress-true strain relationship over a significant strain range.

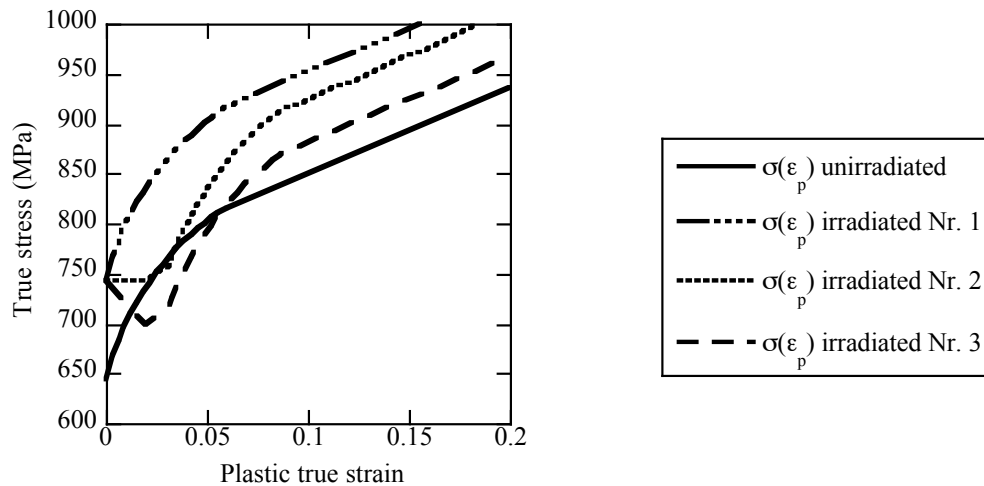


FIG 5. Four different constitutive behaviors used as input to simulate the stress field at a crack tip.

Table I Applied stress intensity factor K to reach the selected cleavage criterion σ^*-A^*

Constitutive relationship	Applied K to reach: $\sigma^* = 2000 \text{ MPa} - A^* = 1 \times 10^{-8} \text{ m}^2$
$\sigma(\varepsilon_p)$ unirradiated	$100 \text{ MPa m}^{1/2}$
$\sigma(\varepsilon_p)$ irradiated Nr. 1	$56 \text{ MPa m}^{1/2}$
$\sigma(\varepsilon_p)$ irradiated Nr. 2	$66 \text{ MPa m}^{1/2}$
$\sigma(\varepsilon_p)$ irradiated Nr. 3	$85 \text{ MPa m}^{1/2}$

5. Conclusions

In this paper, we reported new developments for the analysis of small ball punch tests (SPT) as well as on the stress/strain fields at the tip of a stationary crack based upon finite element simulations. We showed that it is possible to reconstruct the entire SPT load-deflection curves. We discussed the influence of the yield stress and of the post-yield behavior on the overall shape of the SPT curve. We concluded that the yield stress, measured by standard tensile tests, can be fairly evaluate through a calibration with the yield load of the SPT curve, independently of the post-yield behavior. A very good estimation of the strain-hardening capacity of the materials after irradiation can also be done by considering the slope of the SPT curves at deflection larger than 0.2 mm. However, a precise determination of the shape of the $\sigma(\varepsilon_p)$ curves is certainly more critical. As far as the fracture toughness is concerned, we studied the influence of the irradiation hardening and of moderate variations in the constitutive behavior on the applied stress intensity factor necessary to reach a local criterion for cleavage. It was found that these moderate variations in the constitutive properties lead to significant ones in fracture toughness. Hence, we identify a real need to better characterize the post-yield behavior of the irradiated specimens and recommend to foresee in the IFMIF irradiation matrices not only tensile specimens but also compression or

torsion ones that would allow precise determination of the strain-hardening in the low to moderate strain range.

Acknowledgments

The Paul Scherrer Institute is acknowledged for providing access to its facilities. This work has been supported by the EFDA Technology Programme. The financial support of the Swiss National Foundation is gratefully acknowledged.

References

- [1] HISHINUMA, A., et al. "Current status and future R&D for reduced-activation ferritic/martensitic steels", *J. Nucl. Mater.* **258-263** (1998) 193.
- [2] RENSMAN, J., et al., "Tensile properties and transition behavior of RAFM steel plate and welds irradiated up to 10 dpa at 300°C", *J. Nucl. Mar.* **307** (2002) 245.
- [3] MARMY, P., et al., "Pirex II – A new irradiation facility for testing fusion first wall materials", *Nucl. Inst. Meth. Phys. Res.* **B47** (1990) 37.
- [4] EHRLICH, K., MÖSLANG, "IFMIF – An international fusion materials irradiation facility", *Nucl. Inst. Meth. Phys. Res.* **B139** (1998) 72.
- [5] MÖSLANG, A., et al., "Suitability and feasibility of the International Fusion Materials Irradiation Facility (IFMIF) for fusion materials studies", *Nucl. Fusion* **40** (2000) 619.
- [6] LUCAS, G.E., "The development of small specimen mechanical test techniques", *J. Nucl. Mater.* **117** (1983) 327.
- [7] LUCAS, G.E., et al., "Recent progress in small specimen test technology", *J. Nucl. Mater.* **307-311** (2002) 1600.
- [8] JUNG, P., et al., "Recommendation of miniaturized techniques for mechanical testing of fusion materials in an intense neutron sources", *J. Nucl. Mater.* **232** (1996) 186.
- [9] MAO, X., TAKAHASHI, H., "Development of a further miniaturized specimen of 3 mm diameter for TEM small punch tests", *J. Nucl. Mater* **150** (1987) 42.
- [10] SONG, S.H., et al., "Temper embrittlement of a CrMo low-alloy steel evaluated by means of small punch testing", *Mater. Sci. Eng. A* **281** (2000) 75.
- [11] CAMPITELI, E.N, et al., "Assessment of the constitutive properties from small ball punch test: experiment and modeling", *accepted in J. Nucl. Mater* (2004).
- [12] BONADE, R., et al., "Plastic Flow of Martensitic Model Alloys", *accepted in Mat. Sci. Engng A* (2004).
- [13] BONADE, R., et al., "Tensile Properties of a Tempered Martensitic Iron-Chromium-Carbon Model Alloy", *J. Nucl. Mater* **329-333** (2004)
- [14] ODETTE, G.R., et al., "Modeling the multiscale mechanics of flow localization-ductility loss in irradiation damaged bcc alloys", *J. Nucl. Mater* **307-311** (2002) 171.
- [15] ODETTE, G.R., "On the ductile to brittle transition in martensitic steels—Mechanisms, models, and structural implications", *J. Nucl. Mat.* **212-215** 45 (1994).
- [16] NEVALAINEN, M., DODDS, R.H., "Numerical investigation of 3-D constraint effects on brittle fracture in SE(B) and C(T) specimens", *Inter. J. Fract.* **74** (1995) 131.
- [17] RITCHIE, R.O., et al., "On the relationship between critical tensile stress and fracture toughness in mild steel", *J. Mech. Phys. Sol.* **21** (1973) 395.
- [18] ODETTE, G.R., et al. "Developing fracture assessment methods for fusion reactor materials with small specimens", *Small Specimen Test Techniques*, ASTM STP 1329
- [19] ODETTE, G.R., "A master curve analysis of F82H using statistical and constraint loss size adjustments of small specimen data", *J. Nucl. Mater* **329-333** (2004) 1243.
- [20] GAO, X., et al. "Calibration of Weibull stress parameters using fracture toughness data" *Inter. J. Fract.* **92** (1998) 175.